15 January 2002

ELSEVIER

Optics Communications 201 (2002) 391–397

OPTICS COMMUNICATIONS

www.elsevier.com/locate/optcom

Frequency noise characterisation of narrow linewidth diode lasers

L.D. Turner, K.P. Weber, C.J. Hawthorn, R.E. Scholten *

School of Physics, University of Melbourne, Parkville, Vic. 3010, Australia

Received 4 October 2001; received in revised form 4 October 2001; accepted 15 November 2001

Abstract

We examine several approaches to laser frequency noise measurement in the frequency and time domains. Commonly employed methods such as optical frequency discrimination and the Allan variance are found to be complex, expensive, time-consuming, or incomplete. We describe a practical method of demodulating a laser beat note to measure a frequency noise spectrum, using a phase-locked loop frequency discriminator based on a single low-cost integrated circuit. This method measures the frequency noise spectrum of a laser directly and in detail and is insensitive to intensity fluctuations. The advantages of this scheme are demonstrated through measurement of the frequency noise spectrum for two external cavity diode lasers (ECDL), clearly distinguishing several common noise sources. These are isolated and removed, reducing the individual laser rms linewidth from 2 MHz to 450 kHz. The spectrum is used to calculate the Allan variance, which shows almost none of the important information.

PACS: 42.55.-f; 42.55.Px; 42.60.Mi; 42.60.-v

Keywords: Diode lasers; Frequency noise; Frequency discrimination

1. Introduction

Narrow linewidth and highly stable lasers are critically important in fields as diverse as optical communications, laser cooling and atomic frequency standards. When designing a laser system, the identification and removal of frequency noise sources is crucial to narrowing the linewidth. Accurate measurement of the laser frequency stability is also often required as an experimental parameter.

External cavity diode lasers (ECDLs) are a common example of such narrow linewidth lasers [1]. ECDLs use semiconductor diode lasers in an external cavity with dispersive feedback, often from a diffraction grating. The linewidth is greatly reduced with respect to the diode alone, and the laser can be tuned through the broad gain curve of the diode.

* Corresponding author. Tel.: +61-3-8344-5457; fax: +61-3-9347-4783.

E-mail address: r.scholten@physics.unimelb.edu.au (R.E. Scholten).

0030-4018/02/$ - see front matter
PII: S0030-4018(01)01689-3

ECDLs exhibit varying forms of frequency noise from environmental, fundamental, and artificial sources. Environmental noise includes 50 or 60 Hz power-line-induced noise, and acoustically coupled noise, in particular at frequencies corresponding to mechanical resonances. Fundamental noise is typically dominated by white phase noise at high frequencies and flicker frequency noise (also known as $1/f$ noise or pink noise) at low frequencies [2]. The flicker frequency noise is often the dominant component of the linewidth, and so it is common practice to stabilise the laser to an external frequency reference, for example a Fabry–Perot etalon or sub-Doppler atomic resonance. The feedback systems usually rely on dithering the laser frequency [3] or the reference frequency [4], but in both cases it is common to find significant noise at the dither frequency, thus introducing an artificial source of frequency noise.

2. Measurement of laser frequency noise

Laser frequency noise may be measured directly at the optical frequency, or by heterodyning to a reference laser.

2.1. Optical frequency discrimination

Direct optical measurements use an optical frequency discriminator to convert frequency modulation to intensity modulation. Common examples are transmission at the side of a Fabry–Perot etalon fringe [5], or the side of an atomic absorption resonance [6], either Doppler-broadened or sub-Doppler. These can be convenient and low cost, but high frequency resolution, signal to noise ratio, and stability are more difficult to achieve. In addition, such optical frequency discriminators typically do not distinguish between frequency and intensity fluctuations. This lack of distinction between the two types of fluctuations is particularly important when analysing the frequency noise of diode lasers, because fluctuations in the injection current affect both frequency and output power.

2.2. Radio frequency discrimination

Laser frequency noise can also be measured by heterodyning two lasers, for example by superimposing the two beams on a fast photodiode (PD) to produce a radio frequency (rf) beat note at the difference frequency. Frequency fluctuations apparent in the beat note are the combination of the individual frequency fluctuations of the lasers. A single laser can also be superimposed with itself via a fiber delay loop [7], but such self-homodyne systems are ill-suited to measuring laser noise at low frequencies, since impracticably long delays are required.

The heterodyne method is very commonly used to obtain a measure of the linewidth of a laser. The beat note is analysed with an rf spectrum analyser and the width of the spectral peak at the beat frequency, averaged over some measurement time, is taken as the combined laser linewidth. Unfortunately this provides very little information on the composition, and hence sources, of the frequency noise [2].

3. Analysis of radio frequency spectra

Frequency noise analysis of the beat signal can provide this information, either in the frequency domain or in the time domain. The beat note signal produced by lasers with frequency difference ν_0 has voltage

$$V(t) = V_0(t)\sin[2\pi\nu_0 + \phi(t)], \tag{1}$$

where $V_0(t)$ describes amplitude fluctuations of the two lasers and $\phi(t)$ is the difference of the individual phases. The instantaneous beat frequency is

$$\nu(t) = \nu_0 + \frac{1}{2\pi}\frac{\mathrm{d}\phi(t)}{\mathrm{d}t} = \nu_0 + \Delta\nu(t) \tag{2}$$

with frequency fluctuations $\Delta\nu(t) \ll \nu_0$.

3.1. Time domain frequency analysis

The time domain parameters are variances of multiple measurements of the instantaneous frequency $\nu(t)$ each of period τ. The standard measure is the Allan variance, the zero dead-time two-sample deviation over a given time period τ:

$$\sigma^2(\tau) = \frac{1}{2}\left\langle [v_\tau(t) - v_\tau(t+\tau)]^2 \right\rangle, \quad (3)$$

where the brackets $\langle\,\rangle$ denote time averaging. The measurement of an Allan variance requires two frequency counters, a pulse sequencer, and a computer with data acquisition system to calculate the variance at each time interval [8].

3.2. Frequency domain analysis

The fundamental parameter in the frequency domain is the frequency noise power spectral density, measured in $\mathrm{Hz}^2/\mathrm{Hz}$, given by

$$S_{\Delta v}(f) = 2\int_0^\infty \langle \Delta v(t)\Delta v(t+\tau)\rangle \exp(-\mathrm{i}2\pi f\tau)\,\mathrm{d}\tau, \quad (4)$$

where f is termed the Fourier frequency. The root mean square (rms) linewidth Δv_{rms} is then

$$\Delta v_{\mathrm{rms}}^2 = \int_0^\infty S_{\Delta v}(f)\,\mathrm{d}f. \quad (5)$$

The beat note linewidth measured on an rf spectrum analyser is not simply related to the rms linewidth. If the frequency noise spectrum is a delta function, the rf beat spectrum will be approximately rectangular with width of $L = 2\sqrt{2}\Delta v_{\mathrm{rms}}$. If the rf beat spectrum is Gaussian, the full width at half maximum (FWHM) will be $2.35\Delta v_{\mathrm{rms}}$ [9].

The Allan variance may be determined from the frequency noise spectrum $S_{\Delta v}$ by the integral [10]

$$\sigma^2(\tau) = 2\int_0^\infty S_{\Delta v}(f)\frac{\sin^4(\pi f\tau)}{(\pi f\tau)^2}\,\mathrm{d}f \quad (6)$$

but in general *the frequency noise spectrum cannot be determined from the Allan variance* [11]. The frequency noise spectrum is therefore preferable to the Allan variance.

4. Experiment

4.1. Phase-locked loop frequency discriminator

The frequency noise spectrum may be recovered directly from the beat signal with a frequency discriminator which outputs a voltage proportional to $\Delta v(t)$, with minimal dependence on amplitude fluctuations $V_0(t)$. The power spectral density of this voltage, for example acquired with an audio frequency spectrum analyser, is $S_{\Delta v}$.

Previous experiments using discriminators have required complex rf electronics [12] and suffered from poor spectral resolution [13]. We describe a simple frequency discriminator and its application to ECDLs, and demonstrate the increased information over the rf beat spectrum alone and over Allan variance measurements.

We use a single chip phase-locked loop (Philips SA568), which consists of a local voltage controlled oscillator phase-locked to the input signal with a phase detector and feedback loop. The feedback voltage depends on the frequency of the input signal. Unlike previously employed discriminators, this frequency discriminator operates across a broad range of beat note frequencies from 40 to 110 MHz, tracks frequency deviations of up to 10 MHz, and is insensitive to amplitude modulation (20 dB rejection).

Fig. 1 is a schematic of our apparatus. The single frequency output beams from two ECDL [14] are superimposed on a New Focus 1621 photodetector. The beat signal was amplified by 32dB with a wideband MMIC (Agilent MSA-0886) and fed directly into the SA568. Our circuit

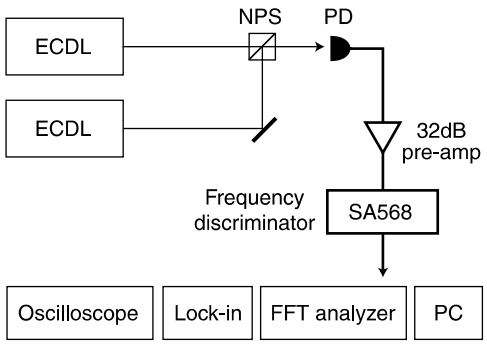

Fig. 1. Two external cavity diode lasers (ECDLs), locked to saturated absorption resonances, were superimposed with a non-polarising beamsplitter (NPS) onto a fast photodiode (PD). The heterodyne signal was pre-amplified and analysed with a frequency discriminator (Philips SA568) and the frequency spectrum acquired with any one of the audio frequency spectrum analysers shown.

uses only a few associated passive components, as specified in the Agilent and Philips datasheets. For normal laboratory use, the frequency discriminator output spectrum can be acquired with an oscilloscope with FFT capability, a lock-in amplifier, or the audio digitiser of a personal computer sound card. For the high-resolution results presented here, we used an SRS760 FFT audio frequency spectrum analyser.

4.2. External cavity diode lasers

The ECDL are based on the Littrow configuration design of Arnold et al. [15] (Fig. 2). Each consists of a Sanyo DL-7140-201 laser diode and aspheric collimating lens ($f = 4.5$ mm 0.55NA, Thorlabs C230TM-B) mounted in a collimation tube (Thorlabs LT230P5-B) fixed to a modified mirror mount (Newport U100-P). A 10 kΩ thermistor sensor and Peltier thermoelectric cooler (Melcor CP1.4-71-045L, $30 \times 30 \times 3.3$ mm^3) are used to stabilise the diode temperature. A gold-coated diffraction grating provides wavelength-selective feedback. We use Richardson Grating Laboratory 3301FL-330H gratings with 1800 lines/mm on a $15 \times 15 \times 3$ mm^3 substrate, with a typical diffraction efficiency of about 15%. Up to 80% of the intra-cavity power is directly reflected to form the output beam. The grating is attached to the front face of the modified U100-P, which provides vertical and horizontal grating adjustment. A 1 mm thick PZT piezoelectric transducer disk under the grating is used to modify the cavity length for fine frequency tuning. The output beam is reflected from a mirror attached to the grating arm. The double reflection from grating and mirror maintains a fixed output beam direction as the grating angle and lasing wavelength is adjusted [14]. The output power is typically 40 mW at 780 nm, and the wavelength can be tuned discontinuously over a 10 nm range by rotation of the grating alone, and over a wider range with suitable temperature adjustment.

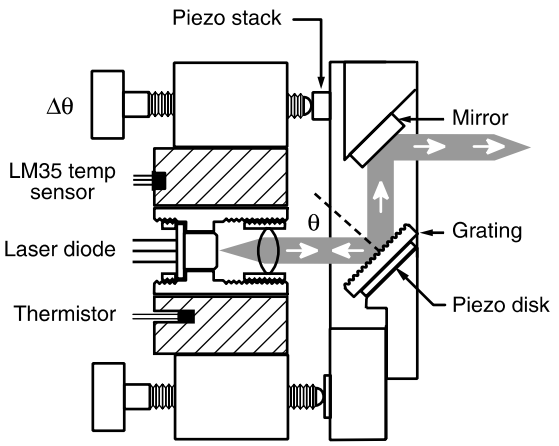

Fig. 2. External cavity diode laser design, based on [15]. An AlGaAs laser diode, aspheric collimation lens, and diffraction grating in a Littrow configuration, are mounted in a kinematic mirror mount. A thermistor temperature sensor is used for feedback to stabilise the laser temperature with a thermoelectric cooler (not shown). An LM35 semiconductor sensor provides a separate temperature readout. The mirror maintains a fixed output beam direction as the grating angle is adjusted [14]. A piezoelectric stack is used to adjust the grating angle and hence wavelength (20 GHz/100 V) and a piezo disk adjusts the cavity length for frequency locking feedback.

The lasers also have a stacked piezoelectric transducer (Tokin AE0203D04) which drives the grating–mirror pivot arm. This stack alters the grating angle and the cavity length, allowing electronic wavelength adjustment of 20 GHz over the 100 V range of the stack. This allows greater scanning range and much safer voltages compared to the original design [15].

Each laser is mounted to a heavy (5 kg) metal base to provide inertial and thermal damping. The base is isolated from the optical bench with viscoelastic polymer (Sorbothane) at the corners and enclosed with an aluminum cover, which is also isolated from the laser by strips of Sorbothane. The laser and saturated absorption optics are covered with an acrylic enclosure. The aluminum cover and acrylic enclosure shield the lasers from air currents, improve temperature stability, and suppress acoustic vibrations.

The laser frequencies were stabilised to two saturated absorption peaks in a rubidium vapour cell using ac (heterodyne) locking [3]. The laser frequencies were initially dithered at 23 and 29 kHz by modulation of the piezo disk voltage. The saturated absorption signals are detected with silicon photodetectors (Burr-Brown OPT210) and a home-made lock-in amplifier. One laser was

locked to the Rb^{85} $5S_{1/2}(F=2) \rightarrow 5P_{3/2}(F'=3)$ hyperfine transition and the other to the Rb^{85} $5S_{1/2}(F=2) \rightarrow 5^2P_{3/2}(F'=2,3)$ crossover, separated by 60.35 MHz.

4.3. Frequency noise spectra

The rf beat between the two lasers was measured with an rf spectrum analyser (Fig. 3), and with our phase-locked loop frequency discriminator (Fig. 4). Once the SA568 internal oscillator frequency was set to within a few MHz of the beat frequency, no further adjustments were necessary. The SA568 output was analysed with the FFT spectrum analyser to produce the frequency noise spectra shown in Fig. 4.

The modulator voltage output per unit frequency deviation input was calibrated by the Bessel null method [16] in which absolute frequency deviations are measured by viewing carrier suppression on an rf spectrum analyser. This calibration is not required for general application, where only the relative contribution of frequency noise sources in a laser system is needed. Even if absolute quantitation is desirable, the rf spectrum analyser is necessary only for a once-off calibration.

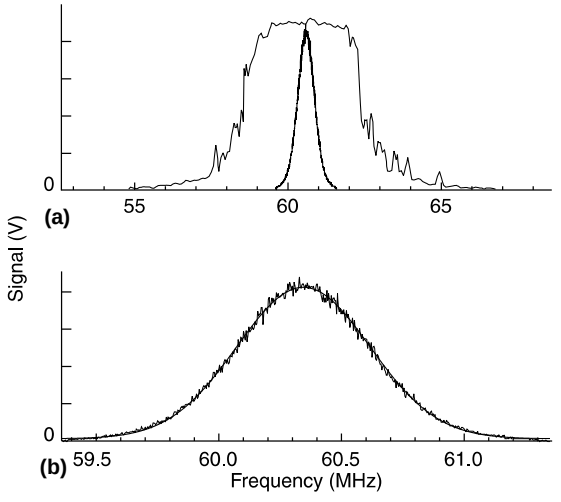

Fig. 3. (a) Beatnote spectra for two ECDLs locked to Rb transitions at 780 nm, separated by 60.3 MHz, before and after noise minimisation modifications. (b) Detail of the beatnote spectrum after noise minimisation modifications, taken with 3 kHz resolution bandwidth, averaged over 64 sweeps of 2 s each. The close agreement with a Gaussian fit (smooth curve) indicates that the deviations in laser frequency are large compared to the frequencies of modulation [9].

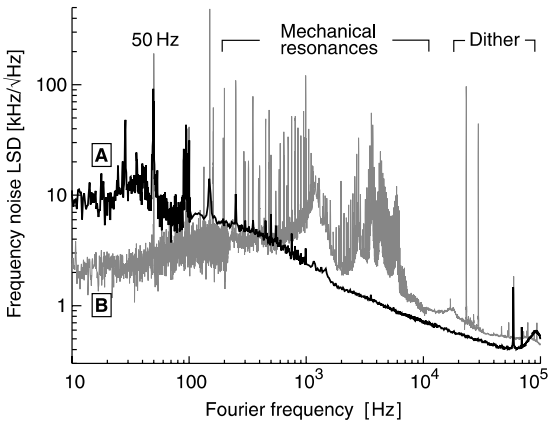

Fig. 4. Frequency noise linear spectral density (the square-root of the power spectral density $S_{\Delta\nu}(f)$) of ECDL beat note, before (B) and after (A) noise minimisation modifications.

The detail evident in the spectra of Fig. 4 immediately illustrates the power of this method. The prominent peaks at 50 and 150 Hz in spectrum (B) are power-line harmonics which are evident up to 6 kHz. The sharp resonance at 990 Hz is due to a turbo-pump on the same optical bench as the experiment. The broad resonance around 1100 Hz is an acoustic mode of the aluminum laser enclosure, while the series of resonances between 2 and 7 kHz are mechanical modes of the mirror mount on which the laser diode and grating are fixed. Peaks due to the dither imposed on the lasers are clearly resolved at 23 and 29 kHz. The overall $1/f$ character is apparent above the bandwidth limit of our control loop ($f > 2$ kHz).

Integrating frequency noise spectrum B using Eq. (5), we find $\Delta\nu_{\mathrm{rms}} = 1.05$ MHz. The rf beat spectrum (Fig. 3(a)) is approximately rectangular, hence we expect a FWHM linewidth of $L = 2\sqrt{2}\Delta\nu_{\mathrm{rms}} = 2.97$ MHz, which is consistent with the measured results. This corresponds to individual laser linewidths of 2 MHz.

Similarly, the relative contribution of the dither and the mechanical modes may be assessed by integrating over the appropriate range of Fourier frequencies. The two dither contributions are 0.6

and 0.15 MHz^2, and the total contribution of mechanical modes and power harmonics for both lasers was 0.2 MHz^2. The square root of the sum of these almost completely accounts for the total rms linewidth.

4.4. Allan variance

Fig. 5 shows the Allan variance of the beat note calculated using Eq. (6). Very little spectral detail is evident. The oscillations at $\tau > 10$ ms are due to the 50 and 150 Hz harmonics of the power line. Oscillations due to the dither for τ between 10 and 100 μs are barely discernible. The resolution of subtle fluctuations due to the dither would require prohibitively large numbers of frequency counts at every delay. The region between 0.1 and 10 ms corresponds to the mechanical modes. Here the Allan variance is amorphous, showing none of the rich structure of Fig. 4. Due to the need to make a large number of counts for every period, determining an Allan variance spectrum is a laborious process, especially for long periods (low frequencies). In contrast, a frequency noise spectrum such as Fig. 4 may be obtained in seconds.

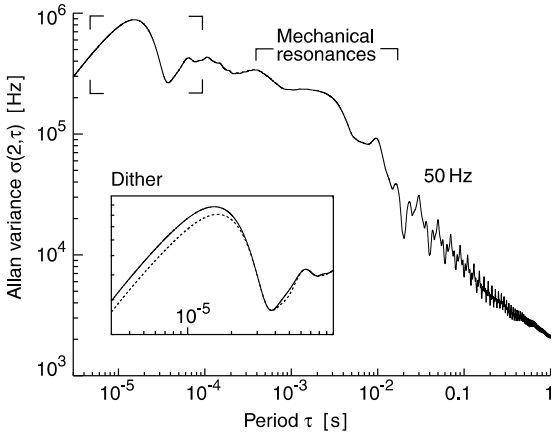

Fig. 5. Allan variance calculated from frequency noise data in Fig. 4. The inset shows an expanded view with an added curve (dashed) calculated from a frequency noise spectrum from which the higher frequency dither peak has been deleted (···). The two variances are almost indistinguishable, whereas in Fig. 4 the dither peaks are clearly resolved.

4.5. Distinguishing and eliminating noise sources

The rf beat spectrum of Fig. 3 is a useful measure of laser performance, but provides little insight into the sources of laser noise. In contrast, the detailed laser frequency noise spectrum of Fig. 4 allows identification of the primary sources of laser noise, such as the power-line harmonics, turbo-pump, dither modulation, and mechanical noise. By distinguishing these separate components, it was possible to systematically reduce each noise source.

The power-line harmonics were minimised by careful elimination of ground loops. Changes to the ground circuits produced changes in the laser frequency noise which were readily apparent in real time from the demodulated spectrum.

The turbo-pump-induced noise was only a small contribution to the total laser linewidth, but was nevertheless eliminated by relocating the lasers to a separate optical table.

The dither modulation frequency noise, caused by modulation of the cavity length via the piezo disk, was reduced by locking to a modulation of the atomic reference frequency rather than the laser [4]. The atomic absorption resonance frequency was modulated by the Zeeman effect, using solenoid coils around our vapour cells. The locking electronics did not completely demodulate the dither frequencies, and hence produced small modulations of the lasers as seen from the peaks in the final laser noise spectrum, at the new dither frequencies of 57 and 68 kHz.

The mechanical noise was investigated by systematically modifying various components of the laser, for example by adding small masses or inelastic damping to the grating, the mirror mount arm, and the retaining springs of the mirror mount. These changes produced frequency shifts of different noise peaks which allowed identification of the mechanical noise sources. Through these explorations, it became apparent that the grating arm and associated retaining springs of the mirror mount were the primary source.

The lasers were initially stabilised by feedback to the piezo stack, which tunes the laser by rotation of the grating, causing a frequency shift of 200 MHz/V. The stack was driven by a high-voltage

(150 V) amplifier with a gain of 10, leading to a net amplification of 2 MHz/mV from the feedback circuit. Thus, the initial laser linewidth of 2 MHz is consistent with just 1 mV of noise in the feedback circuit.

The stack-induced mechanical noise was minimised by connecting the high-voltage feedback to the piezo disk rather than the stack. This reduced the laser linewidth to 400 kHz, but unfortunately also reduced the scanning range of the laser to approximately 1.3 GHz. A regulated and filtered variable dc supply was applied to the stack to allow laser frequency offset adjustment and hence recover the broad tuning range, with only a small penalty in the linewidth.

The final rf beat and frequency noise spectra are shown in Figs. 3 and 4. From the rf beat spectrum, the combined FWHM linewidth has been reduced from 3 MHz to 640 kHz, consistent with individual laser linewidth reductions from 2 MHz to 450 kHz. Integrating the frequency noise spectrum (Eq. (5)), we find $\Delta\nu_{\mathrm{rms}} = 540$ kHz corresponding to a FWHM linewidth of 635 kHz, in excellent agreement with the rf width.

The final linear spectral density noise of Fig. 4 has increased by approximately 5 dB at low frequencies, but is substantially smaller over most of the spectral range. The increased noise at low frequencies is due to a limitation of the simple feedback servo circuit which used only an integrator, leading to excessive gain at low frequencies. While a more complex circuit could reduce this noise, we expect that even if the noise in this band was completely eliminated, each laser linewidth would be reduced by just 70 kHz.

5. Conclusion

These results show that phase-locked loop frequency discrimination provides an unambiguous and high-resolution frequency noise spectrum using common laboratory test equipment. The frequency discriminator separates frequency noise from intensity noise, which is particularly valuable in characterising diode laser systems. In contrast with Allan variance analysis, electronic, mechanical and acoustic noise sources may be clearly identified and observed in real time. The method is applicable to lasers stabilised by electronic and by optical means and is capable of analysing lasers with linewidths from 10 MHz down to a few kHz.

Acknowledgements

We would like to thank Zivko Jovanovski for his expert construction and testing of the radio frequency electronics. This work was supported by the Australian Research Council and conducted with the assistance of the Australian Postgraduate Award scheme (LDT, KPW, CJH).

References

[1] C.E. Wieman, L. Hollberg, Rev. Sci. Instrum. 62 (1991) 1.
[2] Y. Salvadé, R. Dändliker, J. Opt. Soc. Am. A 17 (2000) 927.
[3] A. Hemmerich, D.H. McIntyre, J.D. Schropp, D. Meschede, T.W. Hansch, Opt. Commun. 75 (1990) 118.
[4] T.P. Dinneen, Ch.D. Wallace, P.L. Gould, Opt. Commun. 92 (1992) 277.
[5] M. Kourogi, M. Ohtsu, Opt. Commun. 81 (1991) 204.
[6] A.P. Willis, A.I. Ferguson, D.M. Kane, Opt. Commun. 122 (1995) 31.
[7] H. Ludvigsen, M. Tossavainen, M. Kaivola, Opt. Commun. 155 (1998) 180.
[8] S. Kunze, S. Wolf, G. Rempe, Opt. Commun. 128 (1996) 296.
[9] D.S. Elliott, R. Roy, S.J. Smith, Phys. Rev. A 26 (1982) 12.
[10] J. Rutman, F.L. Walls, Proc. IEEE 79 (1991) 952.
[11] C.A. Greenhall, Does Allan variance determine the spectrum?, in: IEEE International Frequency Control Symposium, Institute of Electrical and Electronics Engineers, New York, 1997.
[12] C.-C. Chen, M.Z. Win, IEEE Photon. Technol. Lett. 2 (1990) 772.
[13] K.R. Manes, A.E. Siegman, Phys. Rev. A 4 (1971) 373.
[14] C.J. Hawthorn, K.P. Weber, R.E. Scholten, Rev. Sci. Instrum. 72 (2001) 4477.
[15] A.S. Arnold, J.S. Wilson, M.G. Boshier, Rev. Sci. Instrum. 69 (1998) 1236.
[16] M. Schwartz, Information Transmission, Modulation, and Noise, McGraw-Hill, New York, 1990.